Integrin αvβ3–associated DAAM1 is essential for collagen-induced invadopodia extension and cell haptotaxis in breast cancer cells

Ting Yan[‡1], **Ailiang Zhang**[§1], **Fangfang Shi**[¶], **Fei Chang**[‖], **Jie Mei**[‖], **Yongjian Liu**[‖], and **Yichao Zhu**[‖**2]

From the ‡*Safety Assessment and Research Center for Drug, Pesticide, and Veterinary Drug of Jiangsu Province, the* ‖*Department of Physiology, and the* **State Key Laboratory of Reproductive Medicine, Nanjing Medical University, Nanjing 211166, China, the* §*Department of Spine Surgery, Third Affiliated Hospital of Soochow University, Changzhou 213003, China, and the* ¶*Department of Oncology, Zhongda Hospital Southeast University, Nanjing 210009, China*

Edited by Eric R. Fearon

The formin protein dishevelled-associated activator of morphogenesis 1 (DAAM1) polymerizes straight actin filaments and mediates migration of cancer cells. However, how DAAM1 governs cell haptotaxis in response to collagen remains unexplored in breast cancer cells. We hypothesized that DAAM1 mediates invadopodia extension and cell haptotaxis in response to type IV collagen in association with integrin receptors. Using Boyden chamber membranes coated with type IV collagen, we show here that type IV collagen activates both DAAM1 and Ras homolog family member A (RHOA) and promotes haptotaxis of MDA-MB-231 and MDA-MB-453 breast cancer cells, a process abolished by treatment with the integrin αvβ3 inhibitor cyclo(-RGDfK). shRNA-mediated knockdown of DAAM1 or a dominant-negative DAAM1 mutation (N-DAAM1) significantly decreased collagen-induced RHOA activity and the assembly of stress fibers, invadopodia extension, and cell haptotaxis. Immunoprecipitation and pulldown assays revealed that integrin αvβ3 is associated with, but only indirectly binds to, the C-terminal DAD domain of DAAM1 in mammalian cells. Blockade of RHOA activation with a specific inhibitor (CCG-1423) or via a dominant-negative RHOA mutation (RHOA-N19) suppressed collagen-induced invadopodia extension and haptotaxis of the MDA-MB-231 and MDA-MB-453 cells. Immunoblotting and immunofluorescence assays indicated high DAAM1 and RHOA expression in invadopodia, which was abolished by cyclo(-RGDfK) treatment or DAAM1 knockdown. These findings have uncovered an integrin αvβ3/DAAM1/RHOA signaling pathway for type IV collagen–induced invadopodia extension and haptotaxis in breast cancer cells. Targeting this pathway may be a means for reducing invasiveness and metastasis of breast cancer.

Although metastases of epithelial cancers are responsible for 90% of human cancer-related deaths, the mechanisms regulating the development and metastasis of carcinomas are not fully understood. Haptotaxis, a motility directed by a gradient of cellular adhesion sites or substrate-bound chemoattractants, frequently occurs at the early stage of epithelial tumor metastasis (1). During haptotaxis, cancer cells are guided by gradients of surface-bound extracellular matrix (ECM)[3] proteins (2).

ECM is composed of highly diverse and dynamic components that regulate cell activities. Fibrillar collagens, fibronectin, hyaluronan, and matricellular protein are matrix components commonly found in involution and cancer (3). ECM serves as an adhesive substrate for cell migration and, by binding morphogens and growth factors, creates concentration gradients for haptotactic migration or pattern formation (4, 5). ECM protein rich in laminin and type IV collagen makes up the specialized basement membrane that provides a barrier for cell invasion and substrates for adhesion of migrating tumor cells (6). The initial phases of tumor cell invasion and migration require transducing extracellular signaling from the surrounding ECM to trigger the intracellular signaling controlling motility.

Integrins are a family of 24 αβ heterodimeric transmembrane cell-surface receptors that modulate cell behavior, transducing spatiotemporal messages from the extracellular environment (7). The roles of collagen-binding integrins in physiological and pathological settings emphasize wound healing, fibrosis, and tumor–stroma interactions (8–10). Dysregulation of integrin αvβ3 expression and/or signaling correlates with development of cancer (*e.g.* promoting epithelial–mesenchymal transition, mediating metastasize to bone, and modulating cell adhesion and invasion) (11–13). Although recent literature reports that integrin αvβ3 activates intracellular kinases to regulate the motile behavior of tumor cells (13, 14), little is known about which novel molecule interacts with integrin αvβ3 and then modulates cellular actin cytoskeleton.

[3] The abbreviations used are: ECM, extracellular matrix; EGFP, enhanced green fluorescent protein; HA, hemagglutinin; GTPγS, guanosine 5′-3-*O*-(thio)triphosphate; GAPDH, glyceraldehyde-3-phosphate dehydrogenase; DAPI, 4′,6-diamidino-2-phenylindole; TRITC, tetramethylrhodamine isothiocyanate.

Invadopodia are actin-rich protrusions of the plasma membrane that are associated with degradation of the ECM in cancer invasiveness and metastasis (15). Actin polymerization is crucial for the formation and function of invadopodia. Formin proteins, elements of the cellular actin cytoskeleton, can polymerize actin filaments at the barbed end (16). Based on their sequences and domain architectures in mammals, a total of 15 formin proteins are grouped into eight different subfamilies (17). The protein dishevelled-associated activator of morphogenesis 1 (DAAM1) is an autoinhibited formin protein. DAAM1 is identified as an interaction factor of dishevelled (Dvl) and mediates the noncanonical Wnt/PCP (planar cell polarity) signaling pathway (18, 19). Our previous study finds that active DAAM1 is the downstream target of Wnt5a/Dvl2, and its activation is required for Wnt5a-induced cell migration (19). Here, we report that DAAM1 is associated with integrin $\beta3$ and then promotes invadopodia extension and cell haptotaxis in response to type IV collagen. These results reveal the molecular signaling mechanism in the haptotaxis of breast cancer cells and identify DAAM1 as a target for anticancer therapy.

Results

Type IV collagen induces haptotaxis of breast cancer cells

To determine whether collagen induced directional cell haptotaxis, we examined the migration of MDA-MB-231 for 8 h in 8.0-μm porous Boyden chamber membranes coated with 0, 1, 5 10, or 20 μg/ml type IV collagen on the lower sides of membranes, respectively. Ten and 20 μg/ml type IV collagen largely elevated the haptotaxis of MDA-MB-231 cells (Fig. S1). Next, we tested the migration of MDA-MB-231 and MDA-MB-453 breast cancer cells and MCF10A mammary epithelial cells through 8.0-μm porous membranes coated with vehicle or 10 μg/ml type IV collagen on the upper sides, both sides, or lower sides. An approximately 15-fold increase was observed in the number of migrant breast cancer cells induced by type IV collagen coated on the lower sides compared with that of vehicle groups (Fig. 1, *A–C*). Moreover, a 3-fold increase was observed in the number of migrant breast cancer cells induced by type IV collagen coated on the lower sides compared with that of both-side–coated groups (Fig. 1, *A–C*). A comparison of migrant MCF10A cells in the Boyden chamber membranes coated with collagen on both sides with those in the Boyden chamber membranes coated with collagen on the lower sides revealed that collagen-induced haptotaxis only exists in breast cancer cells (Fig. 1, *A* and *D*). In addition, collagen coated on the upper sides exhibited little effect on cell migration of both breast cancer cells and mammary cells (Fig. 1, *A–D*). To exclude the effect of Wnt5a on cell migration under the condition of collagen-coated Boyden chamber membranes, we examined the secretion of Wnt5a in MDA-MB-231 and MDA-MB-453 cells seeded on coverslips coated with type IV collagen (10 μg/ml) or vehicle. MDA-MB-231 and MDA-MB-453 cells exhibited low endogenous secretion of Wnt5a, which was not statistically changed under collagen-treated conditions (Fig. S2). Accordingly, 10 μg/ml type IV collagen treated for 8 h was used to identify the mechanism for the haptotaxis in breast cancer cells.

DAAM1 is involved in collagen-induced cell haptotaxis

For oriented cell migration, dishevelled and DAAM1 are recruited in the reorganization of actin cytoskeleton (19, 20). We examined whether DAAM1 also mediated collagen-induced haptotaxis of breast cancer cells. Pulldown assays and immunoblotting showed a significant elevation of active DAAM1 levels after 4-h induction by type IV collagen (Fig. 1, *E–G*). Moreover, the active DAAM1 of cells in Boyden chamber membranes coated with collagen on the lower sides was further increased compared with that in Boyden chamber membranes coated with collagen on the upper side and both sides (Fig. 1, *E–G*). To analyze the role of endogenous DAAM1 activation in collagen-induced haptotaxis, we knocked down DAAM1 expression using shRNA using shRNA (#1 and #2) and selected the stable DAAM1 knockdown cells (Fig. 1*H*). shRNA targeting DAAM1 reduced the protein levels of DAAM1 by more than 80% (Fig. 1*H*). The haptotaxis of stable DAAM1 knockdown cells was significantly retarded after the induction of type IV collagen coated on the lower sides of Boyden chamber membranes (Fig. 1, *I* and *J*). Moreover, full-length DAAM1 cDNA with three mutation sites that could be unpaired with DAAM1 shRNA #2 rescued the haptotaxis of DAAM1-knockdown breast cancer cells (Fig. S3). We also transiently transfected a panel of DAAM1 truncations into MDA-MB-231 and MDA-MB-453 cells and tested their roles in cell haptotaxis. To measure the percentage of the transfected cells, we co-transfected DAAM1 truncations with an EGFP construct. The expression efficiency of EGFP puncta was 60–70% as observed under a fluorescence microscope. Interestingly, the expression of full-length endogenous DAAM1 is down-regulated by the expression of C-DAAM1 (C-terminal of DAAM1), but not by N-DAAM1 (dominant-negative DAAM1) (Fig. 1, *K, N,* and *P*). N-DAAM1 retarded collagen-induced cell haptotaxis (Fig. 1, *L* and *M*), whereas C-DAAM1 failed to accelerate cell haptotaxis (Fig. 1, *N* and *O*). Taken together, these experiments demonstrated that active DAAM1 is involved in collagen-induced haptotaxis of breast cancer cells.

DAAM1 acts as a downstream target of integrin and is associated with integrin $\alpha v\beta3$

To determine whether integrin receptor mediated collagen-induced directional haptotaxis, we examined the migration of MDA-MB-231 or MDA-MB-453 cells through 8.0-μm porous membranes coated with type IV collagen on the lower side after treating with integrin inhibitors. Large decreases were observed in the number of migrant cells incubated with cilengitide trifluoroacetate (an integrin inhibitor for $\alpha v\beta3$ receptor and $\alpha v\beta5$ receptor) or cyclo(-RGDfK) (a specific inhibitor for integrin $\alpha v\beta3$) (Fig. 2*A*), suggesting that $\alpha v\beta3$ integrin mediated collagen-induced cell haptotaxis. To examine whether integrin regulated DAAM1 in breast cancer cells, we measured the activity of DAAM1 after treating MDA-MB-231 or MDA-MB-453 cells with cyclo(-RGDfK). We found a significant decrease of DAAM1 activity in the presence of the $\alpha v\beta3$ integrin inhibitor (Fig. 2, *B* and *C*). These data strongly implicated $\alpha v\beta3$ integrin in collagen-induced DAAM1 activation and haptotaxis of MDA-MB-231 and MDA-MB-453 cells.
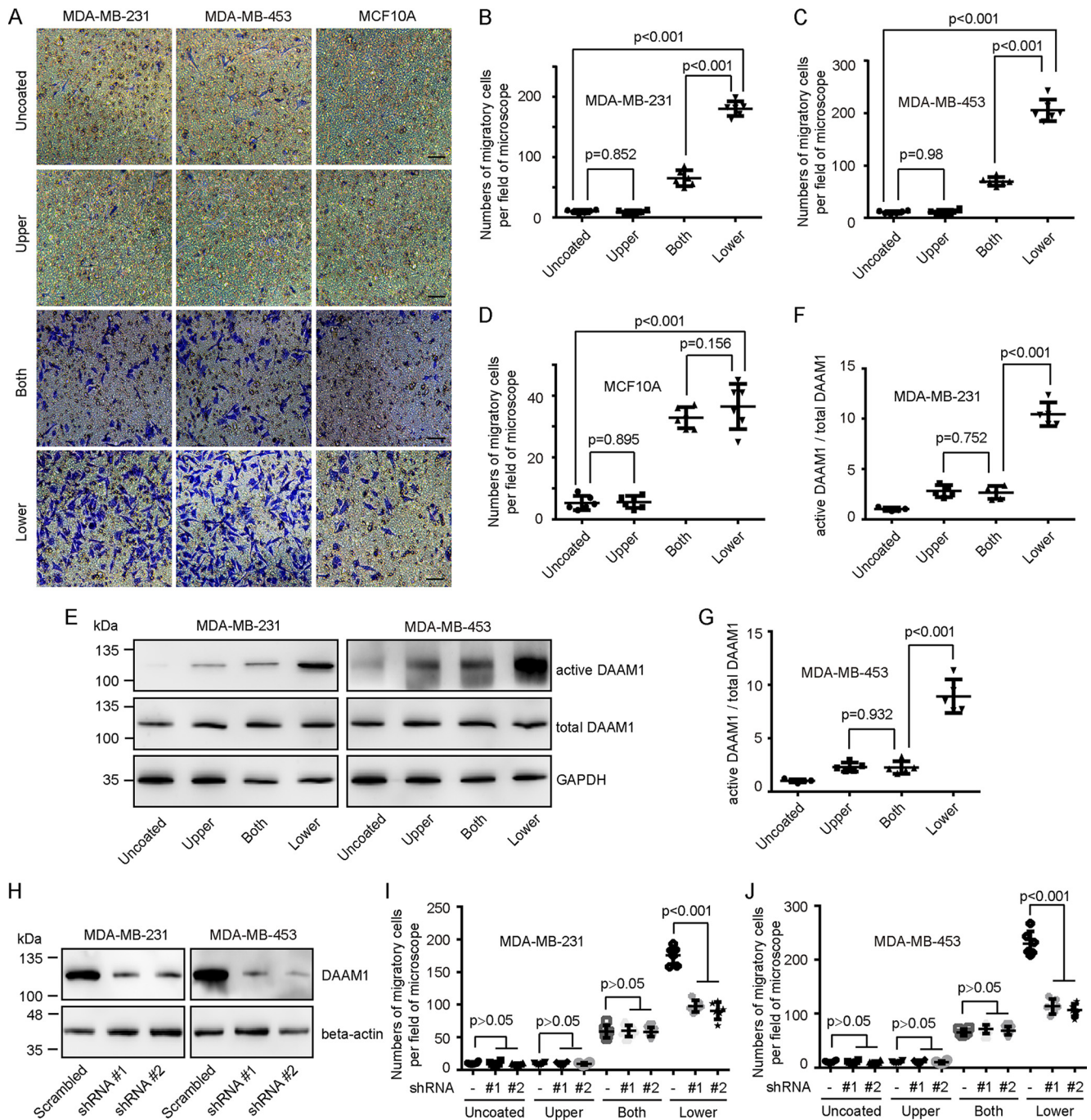
Figure 1. DAAM1 activation is required for collagen-induced cell haptotaxis. *A–D*, type IV collagen triggered haptotaxis of MDA-MB-231 and MDA-MB-453 breast cancer cells. MDA-MB-231, MDA-MB-453, and MCF10A cells were examined for cell haptotaxis for 8 h in 8.0-μm porous Boyden chamber membranes coated with vehicle (*Uncoated*) or type IV collagen on upper sides (*Upper*), both sides (*Both*), or lower sides (*Lower*). Migratory cells on the lower side of the membrane were counted per field of the microscope. *Bar*, 50 μm. Objective lens, magnification, ×20; numerical aperture, 0.75. *E–G*, DAAM1 activation was significantly elevated by type IV collagen coated on the lower sides of Boyden chamber membranes. MDA-MB-231 or MDA-MB-453 cells were seeded on Boyden chamber membranes coated with vehicle (*Uncoated*) or type IV collagen on upper sides (*Upper*), both sides (*Both*), or lower sides (*Lower*). MDA-MB-231 or MDA-MB-453 cells were allowed to migrate toward collagen for 4 h. Cellular lysates were assayed for the active DAAM1 by a pulldown assay using a GST-RHOA as a bait. *H*, efficiency of gene knockdown was analyzed by immunoblotting for DAAM1. MDA-MB-231 and MDA-MB-453 cells were transfected with scrambled or DAAM1 shRNAs (#1 and #2). Total protein extracts from MDA-MB-231 and MDA-MB-453 cells transfected with scrambled or DAAM1 shRNAs were analyzed by immunoblotting for DAAM1. *I* and *J*, knockdown of DAAM1 significantly inhibited cell haptotaxis induced by collagen coated on the lower sides of Boyden chamber membranes. MDA-MB-231 and MDA-MB-453 cells transfected with DAAM1 shRNA or scrambled shRNAs were allowed to migrate for 8 h, and the migration rate was determined by Boyden chamber assays. *K* and *P*, the expression of empty vector and HA-tagged N-DAAM1 (N terminus of DAAM1) was verified using total protein from cells and immunoblotted using anti-HA antibody. The expression level of DAAM1 was tested using immunoblotting and proved the efficiency of N-DAAM1 expression. *L* and *M*, the expression of N-DAAM1 significantly inhibited cell haptotaxis induced by collagen coated on the lower sides of Boyden chamber membranes. MDA-MB-231 and MDA-MB-453 cells transfected with N-DAAM1 were allowed to migrate for 8 h, and the number of migratory cells were counted per field of the microscope. *N* and *P*, the expression of empty vector and HA-tagged C-DAAM1 (C terminus of DAAM1) was verified using total protein from cells and immunoblotted using anti-HA antibody. The expression level of DAAM1 was tested using immunoblotting and proved the efficiency of C-DAAM1 expression. *O*, MDA-MB-231 cells transfected with C-DAAM1 were seeded on Boyden chamber membranes and allowed to migrate for 8 h, and the number of migratory cells were counted per field of the microscope. *Error bars*, S.D.
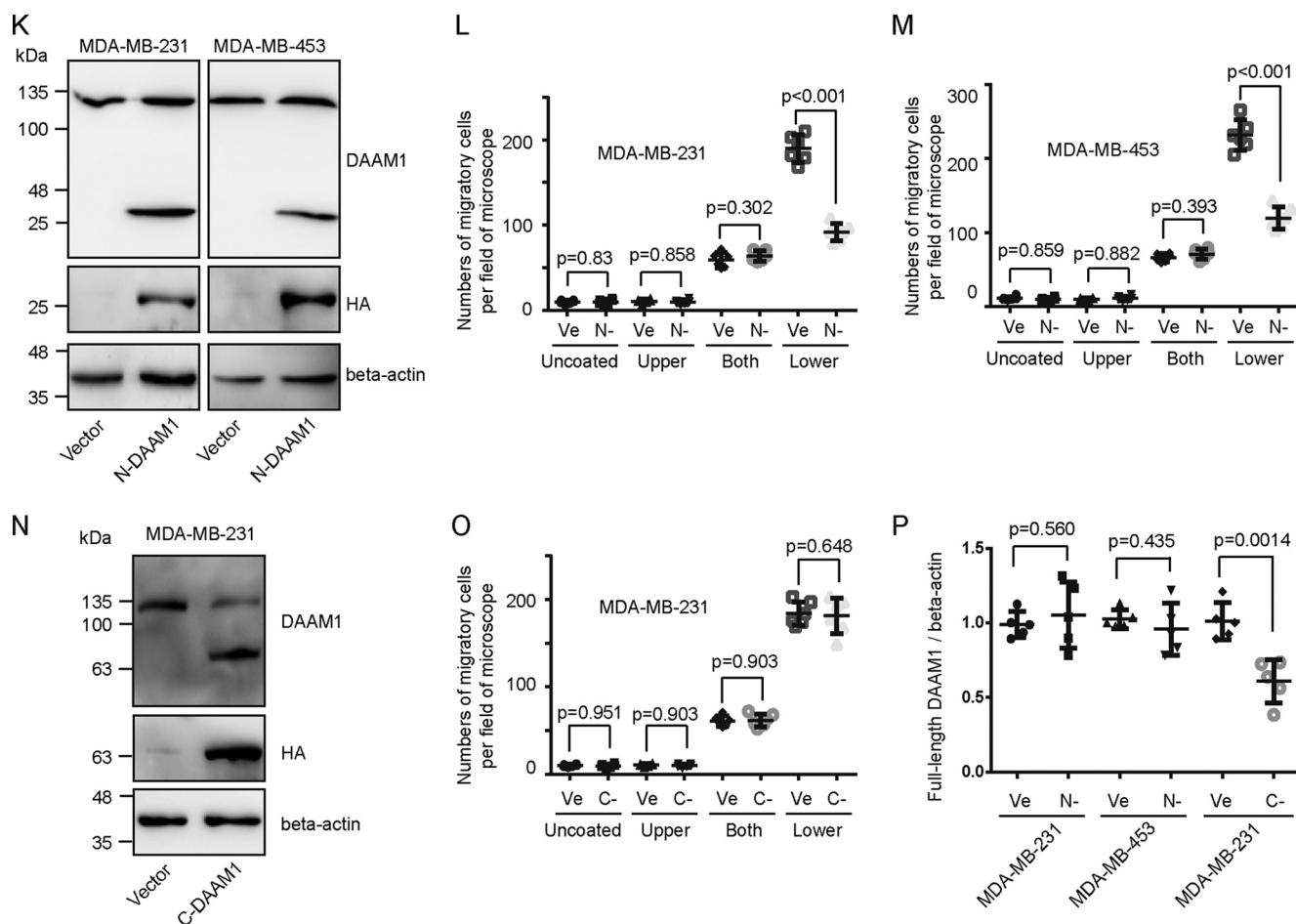
Figure 1—*continued*

Next, we tested whether the physical interaction of DAAM1 with integrin was collagen-dependent in human cancer cells. Interestingly, DAAM1 was strongly associated with integrin $\beta 3$ in MDA-MB-231 or MDA-MB-453 cells, which was enhanced upon collagen type IV stimulation (Fig. 2, *D* and *E*). To test which domain of DAAM1 indeed interacted with integrin $\beta 3$, we expressed HA-tagged DAAM1 constructs in HEK-293T cells followed by immunoprecipitation with anti-HA antibody. Blotting with an HA antibody confirmed the high expression of full-length DAAM1 and truncations (Fig. 2*F*). The immunoprecipitated HA-DAAM1 and C-DAAM1 pulled down integrin $\beta 3$ (Fig. 2*F*). However, the immunoprecipitated HA-ΔDAD-DAAM1 failed to pull down integrin $\beta 3$ (Fig. 2*F*). Using an *in vitro* binding assay, we demonstrated that purified bacterially expressed recombinant DAAM1 did not directly bind to the C-terminal domain of integrin $\beta 3$ (Fig. 2*G*). Thus, we verified that the C-terminal DAD domain of DAAM1 was associated with, but indirectly bound to, integrin $\beta 3$ in mammalian cells.

RHOA acts as a downstream target of DAAM1 and mediates collagen-induced cell haptotaxis

Given that Rho GTPases play a central role in all types of cell migration (21), we suggest that Rho GTPases may promote haptotaxis of breast cancer cells in response to the collagen gradient. Rho GTPase activation assays showed the significantly increased activity of RHOA, Ras-related C3 botulinum

toxin substrate 1 (RAC1), and cell division control protein 42 homolog (CDC42) after 4 h of type IV collagen treatment (Fig. 3, *A–C*). To elucidate which specific Rho GTPases participated in the DAAM1-mediated cell haptotaxis, we performed Rho GTPase activation assays after DAAM1 knockdown. The activation of RHOA, not RAC1 or CDC42, was down-regulated in stable DAAM1 knockdown MDA-MB-231 cells (Fig. 3*D*). Next, we found that RHOA activation was largely inhibited by cyclo (-RGDfK) treatment in MDA-MB-231 cells (Fig. 3*E*). These results indicated that RHOA functioned as a downstream target of integrin $\alpha v\beta 3$/DAAM1 in breast cancer cells.

We used CCG-1423 (a RHOA-specific inhibitor) to study the role of RHOA activation in cell haptotaxis. Preincubation with 1 μmol/liter CCG-1423 for 1 h completely inhibited the haptotaxis of MDA-MB-231 and MDA-MB-453 cells induced by collagen coated on the lower sides of Boyden chamber membranes (Fig. 3, *F* and *H*). Also, we transfected MDA-MB-231 and MDA-MB-453 cells with RHOA-N19 (dominant negative mutant) and selected the stable RHOA-N19–overexpressed cells. Overexpression of N19-RHOA completely abolished the haptotaxis of MDA-MB-231 and MDA-MB-453 cells induced by collagen coated on the lower sides of Boyden chamber membranes (Fig. 3, *G* and *H*). To examine whether RHOA regulated DAAM1 in MDA-MB-231 cells, we measured the activity of DAAM1 in RHOA-N19–overexpressed cells. A comparison of
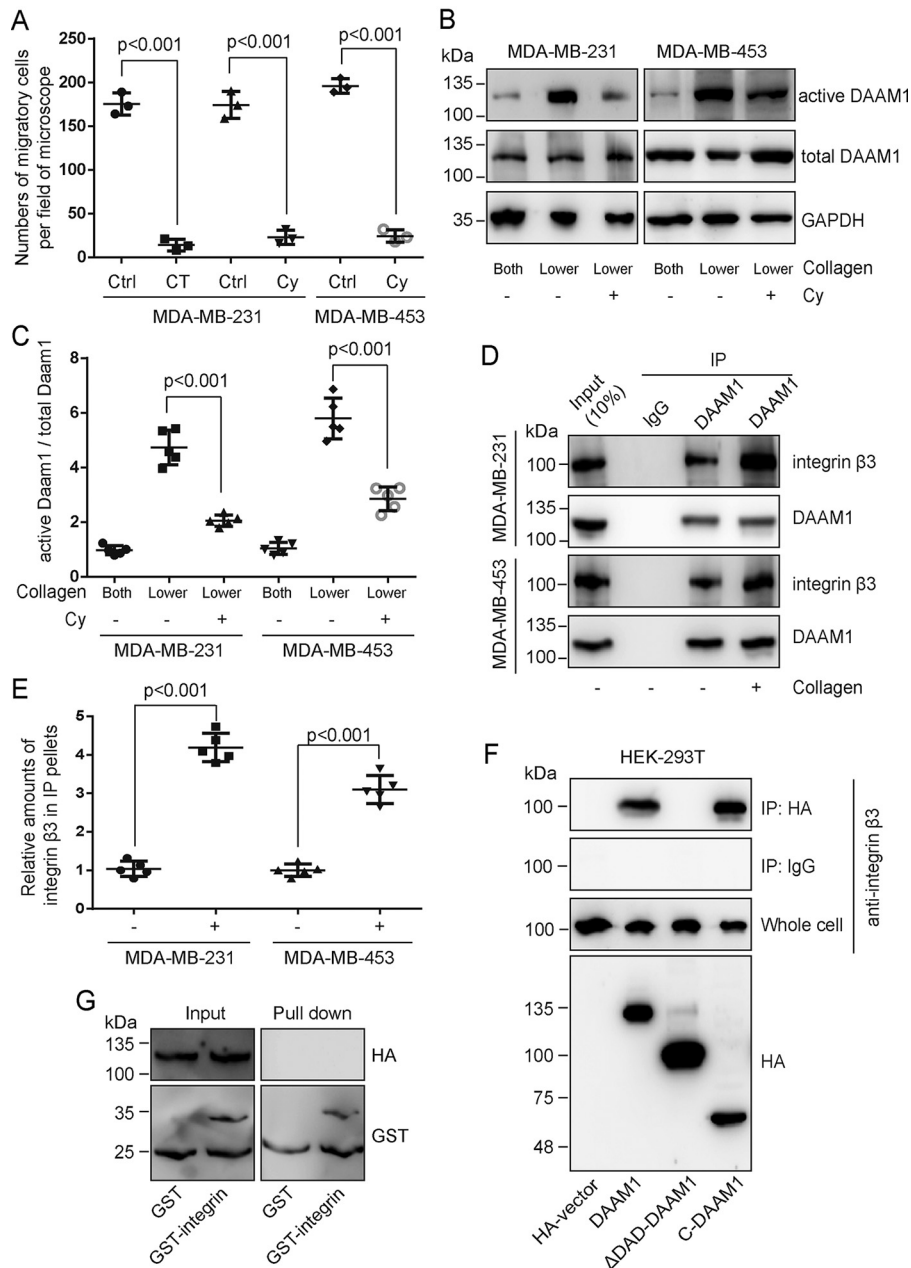
Figure 2. DAAM1 is associated with integrin β3 and acts as a downstream target of the integrin receptor. *A*, integrin inhibitors blocked type IV collagen–induced haptotaxis of breast cancer cells. MDA-MB-231 and/or MDA-MB-453 cells, treated with cilengitide trifluoroacetate (an integrin inhibitor for $\alpha v \beta 3$ receptor and $\alpha v \beta 5$ receptor, 10 nmol/liter) or cyclo(-RGDfK) (an $\alpha v \beta 3$ integrin inhibitor, 20 nmol/liter), were examined for cell haptotaxis for 8 h in 8.0-μm porous Boyden chamber membranes coated with type IV collagen on the lower sides. *CT*, cilengitide trifluoroacetate. *Cy*, cyclo(-RGDfK). *B* and *C*, collagen-induced DAAM1 activation was blocked by $\alpha v \beta 3$ integrin inhibitor treatment. MDA-MB-231 or MDA-MB-453 cells were seeded on Boyden chamber membranes coated with collagen type IV on both sides (*Both*) or lower sides (*Lower*) and treated with cyclo(-RGDfK) (20 nmol/liter). MDA-MB-231 or MDA-MB-453 cells were allowed to migrate toward collagen for 4 h. Cellular lysates were assayed for the active DAAM1 by a pulldown assay using a GST-RHOA as a bait. *Cy*, cyclo(-RGDfK). *D* and *E*, the lysates of MDA-MB-231 or MDA-MB-453 cells were subjected to immunoprecipitation (*IP*) with antibody to DAAM1, followed by immunoblotting with antibody to integrin β3 and DAAM1. *F*, HA-tagged DAAM1 constructs were expressed in HEK-293T cells. Cell lysates were harvested and cleared, and integrin was immunoprecipitated with anti-HA antibodies. Immune precipitates were analyzed by immunoblotting for anti-HA or anti-integrin β3. Whole-cell lysates were used as a control. *G*, purified GST or GST-fused C terminus (amino acids 716 –762) of integrin β3 was incubated with purified HA-tagged full-length DAAM1. The amounts of HA-DAAM1 co-purified with GST or GST-integrin (pulldown) were analyzed by immunoblotting. *Error bars*, S.D.

DAAM1 activity in RHOA-N19–overexpressed cells with that in control cells had no statistical differences in the absence of collagen coated on the lower sides of Boyden chamber membranes (Fig. 3, *I* and *J*). N-DAAM1 largely retarded the haptotaxis of MDA-MB-231 cells, which could be rescued by constitutively active RHOA (RHOA-V14) overexpression (Fig. 3*K*). These results indicated that RHOA acted as a downstream target of

DAAM1. Thus, we concluded that DAAM1/RHOA activation is involved in collagen-induced haptotaxis of breast cancer cells.

DAAM1 is highly expressed in invadopodia and mediates their extension

To determine whether collagen induced invadopodia extension, MDA-MB-231 and MDA-MB-453 cells were seeded onto

3.0-μm porous membranes coated with vehicle or 10 μg/ml type IV collagen on the upper sides, both sides, or lower sides. Collagen coated on the upper sides of Boyden chamber membranes or vehicle was unable to induce invadopodia extension (Fig. 4A). An ~3-fold increase was observed in the invadopodia extension induced by collagen coated on the lower sides compared with that induced by collagen coated on both sides (Fig. 4, A and B). Next, we examined whether DAAM1 mediated collagen-induced invadopodia extension. The stable DAAM1 knockdown cells showed a significant decrease of invadopodia

extension after the induction of type IV collagen coated on the lower sides (Fig. 4, C and E). We also treated MDA-MB-231 and MDA-MB-453 cells with cyclo(-RGDfK) and found that this integrin $\alpha v\beta 3$ inhibitor retarded collagen-induced invadopodia extension (Fig. 4, D and E).

We next tested whether DAAM1 was significantly highly expressed in invadopodia of breast cancer cells in response to collagen. Cell bodies (the top sides of membranes) and invadopodia (the lower sides of membranes) of MDA-MB-231 or MDA-MB-453 cells were mechanically separated. The quality
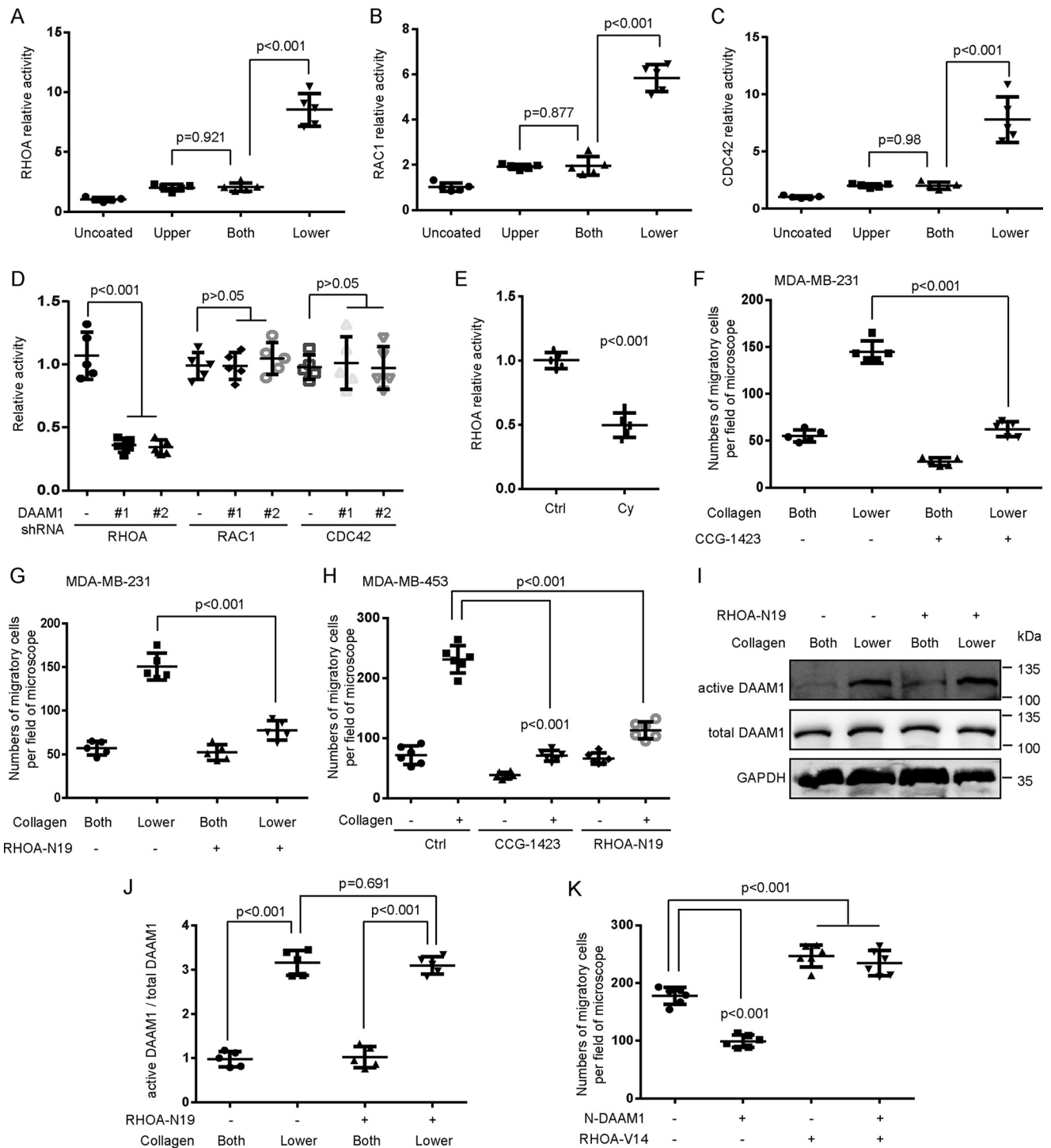
of the fractionation was assessed by immunoblotting for cortactin and histone H3 (Fig. 4F). Indeed, most DAAM1 proteins concentrated in invadopodia of MDA-MB-231 and MDA-MB-453 cells (Fig. 4, F–H). Therefore, we preliminarily demonstrated that active DAAM1 participates in collagen-induced invadopodia extension and is highly expressed in invadopodia of breast cancer cells.

DAAM1-dependent activation of RHOA mediates collagen-induced invadopodia extension

To study the role of RHOA activation in invadopodia extension, we treated breast cancer cells with a RHOA-specific inhibitor (CCG-1423). Preincubation with 1 μmol/liter CCG-1423 for 1 h completely inhibited collagen-induced invadopodia extension in MDA-MB-231 and MDA-MB-453 cells (Fig. 5, A and B). Furthermore, we found that N19-RHOA overexpression completely abolished collagen-induced invadopodia extension (Fig. 5, A and B).

Immunofluorescence showed that RHOA was highly expressed in invadopodia of MDA-MB-231 cells induced by type IV collagen (Fig. 5, C and D). Knockdown of DAAM1 or cyclo (-RGDfK) treatment significantly decreased the number of RHOA-positive invadopodia after collagen induction (Fig. 5, C and D). However, the stable DAAM1 knockdown cells also showed a significant decrease of invadopodia extension (Fig. 4C). We next used a z-axis scan to observe the RHOA location in pores of 3.0-μm porous membranes (Fig. 5, E and F). Knockdown of DAAM1 or cyclo(-RGDfK) treatment significantly blocked the high RHOA expression in invadopodia (Fig. 5, E and F). Thus, we concluded that DAAM1-dependent activation of RHOA mediates collagen-induced invadopodia extension of breast cancer cells.

DAAM1 and RHOA signaling regulate the assembly of stress fibers

We also examined whether DAAM1 and RHOA signaling regulates the assembly of actin filaments in breast cancer cells. We performed fluorescent phalloidin and myosin II staining to investigate the distribution of filamentous actin (F-actin) in MDA-MB-231 cells or stable DAAM1 knockdown cells treated with type IV collagen (Fig. 6A and supporting Fig. S4). We found that the knockdown of DAAM1 disrupted the formation of stress fibers and decreased the length of stress fibers (Fig. 6, A–C). Simultaneously, we also found that CCG-1423 and cyclo(-RGDfK) disrupted the formation of stress fibers and decreased the length of stress fibers (Fig. 6, A–C). Thus, the findings indicated that integrin $\alpha v\beta 3$, DAAM1, and RHOA signaling regulates the assembly of stress fibers in breast cancer cells induced by collagen.

Discussion

The underlying mechanism governing cancer cell haptotaxis remains largely undefined. We conclude that DAAM1 associating with integrin $\alpha v\beta 3$ is indispensable for type IV collagen-induced haptotaxis of breast cancer cells. To exclude the effect of Wnt5a, we examined the secretion of Wnt5a and found that MDA-MB-231 and MDA-MB-453 cells exhibited the low endogenous secretion of Wnt5a, which did not statistically change under collagen-treated conditions. In the previous study (19), the high concentration of Wnt5a (at least 300 ng/ml) was able to induce cell migration of MDA-MB-231 cells. Here, the low endogenous secretion of Wnt5a (<8 ng/ml) is unable to improve cell migration in Boyden chamber assays. Type IV collagen coated on the lower sides of Boyden chamber membranes largely stimulates cell haptotaxis. On the contrary, the small number of cells migrating to the lower component of Boyden chamber membranes coated with collagen on the upper sides reveals that most cells lose their migratory ability and adhere on the upper sides.

DAAM1, a member of formin family, exists in an autoinhibited state with its N-terminal GBD and C-terminal DAD domains intramolecularly interacted (18, 22). Our results show that collagen/integrin $\alpha v\beta 3$ remarkably activates DAAM1 in MDA-MB-231 and MDA-MB-453 cells. Our prior work demonstrates that N-DAAM1 retards Wnt5a-induced cell migration, which is a typical chemotaxis evoked by a chemical stimulus (19). Here, we find that interference with DAAM1 function via N-DAAM1 expression or knockdown of DAAM1 expression via shRNA transfection inhibits RHOA activation and type IV collagen–induced haptotaxis of breast cancer cells. However, the expression of C-DAAM1 does not accelerate collagen-induced haptotaxis. One possible explanation is that the expression of full-length endogenous DAAM1 is down-regulated by C-DAAM1 expression.

Integrins are transmembrane receptors activating signal transduction pathways that mediate cellular signals, such as

Figure 3. RHOA is a downstream target of DAAM1, and its activation is required for collagen-induced cell haptotaxis. *A–C*, RHOA, RAC1, and CDC42 activations were elevated by type IV collagen treatment. MDA-MB-231 cells were seeded on Boyden chamber membranes coated with vehicle (*Uncoated*) or type IV collagen on upper sides (*Upper*), both sides (*Both*), or lower sides (*Lower*). Cells were allowed to migrate toward collagen for 4 h. Cellular lysates were assayed for RHOA, RAC1, and CDC42 activation assays. *D*, collagen-induced RHOA activation was inhibited by DAAM1 silence. Stable DAAM1 knockdown MDA-MB-231 cells (DAAM1 shRNA #1 and #2) and control cells were seeded on Boyden chamber membranes coated with collagen type IV on the lower sides. Cells were allowed to migrate toward collagen for 4 h. Cellular lysates were assayed for RHOA, RAC1, and CDC42 activation assays. *E*, collagen-induced RHOA activation was inhibited by cyclo(-RGDfK) treatment. MDA-MB-231 cells were seeded on Boyden chamber membranes coated with collagen type IV on the lower sides. Cells treated with cyclo(-RGDfK) (20 nmol/liter) were allowed to migrate toward collagen for 4 h. Cellular lysates were assayed for RHOA activation assays. *Cy*, cyclo(-RGDfK). *F* and *G*, CCG-1423 (RHOA-specific inhibitor) or RHOA-N19 (dominant-negative RHOA) inhibited collagen-induced haptotaxis of MDA-MB-231 cells. MDA-MB-231 cells treated with CCG-1423 (1 μmol/liter) or RHOA-N19–overexpressing stable cells were seeded in Boyden chamber membranes coated with type IV collagen on both sides (*Both*) or lower sides (*Lower*). Cells were allowed to migrate toward collagen for 8 h. *H*, CCG-1423 or RHOA-N19 inhibited collagen-induced haptotaxis of MDA-MB-453 cells. MDA-MB-453 cells treated with CCG-1423 (1 μmol/liter) or transfected with RHOA-N19 were seeded in Boyden chamber membranes coated with type IV collagen on both sides (*Both*) or lower sides (*Lower*). Cells were allowed to migrate toward collagen for 8 h. *I* and *J*, DAAM1 activation was not altered by RHOA-N19 overexpression. RHOA-N19–overexpressing stable cells were seeded on Boyden chamber membranes coated with type IV collagen on both sides (*Both*) or on lower sides (*Lower*). Cells were allowed to migrate toward collagen for 4 h. Cellular lysates were assayed for the active DAAM1 by a pulldown assay using a GST-RHOA as a bait. *K*, RHOA-V14 rescued the haptotaxis of N-DAAM1–expressed MDA-MB-231 cells. MDA-MB-231 cells transfected with N-DAAM1 and/or RHOA-V14 were seeded in Boyden chamber membranes coated with type IV collagen on lower sides. Cells were allowed to migrate toward collagen for 8 h. *Error bars*, S.D.
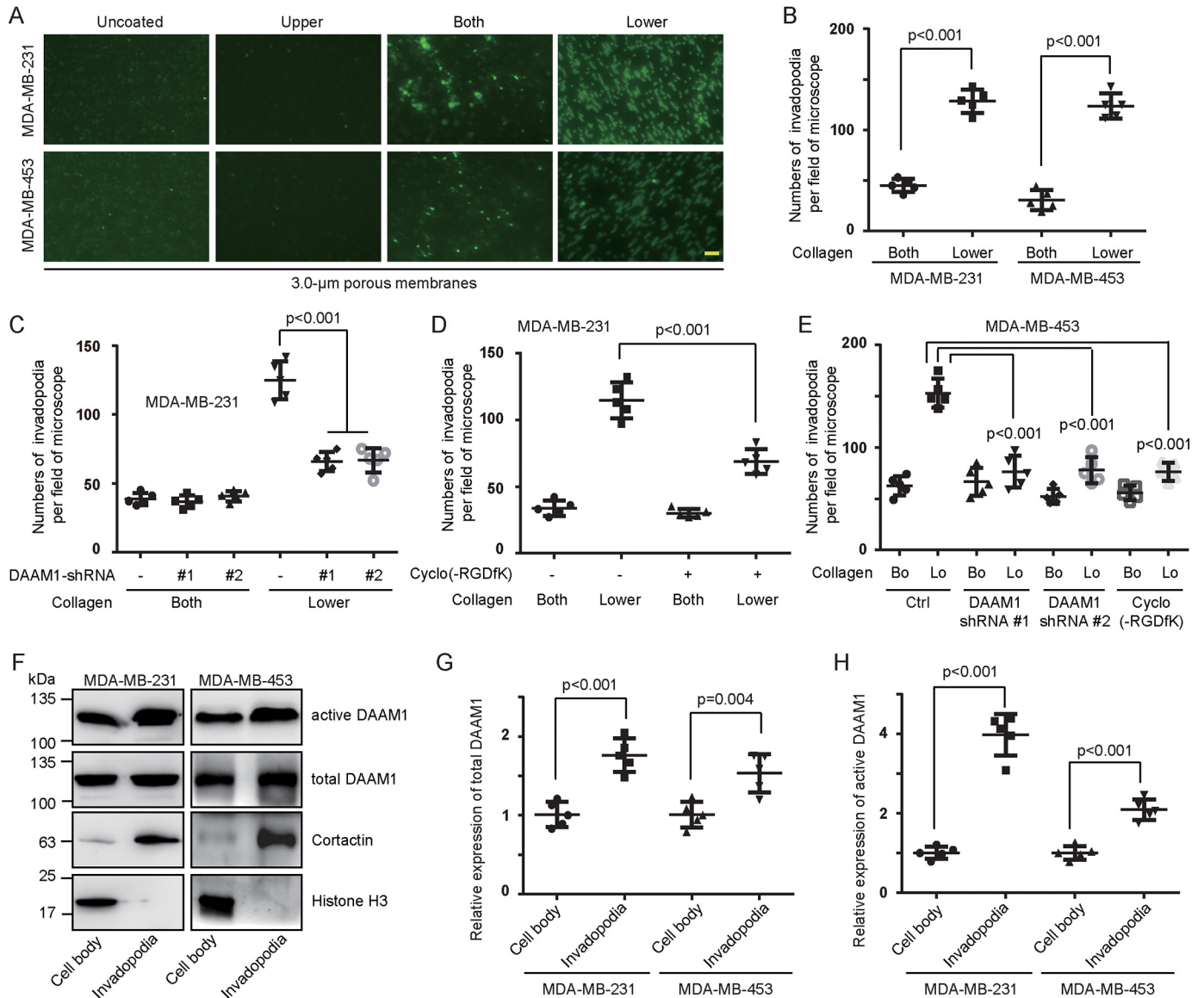
Figure 4. DAAM1 activation is essential for collagen-induced invadopodia extension. *A* and *B*, type IV collagen triggered invadopodia extension of MDA-MB-231 and MDA-MB-453 cells. MDA-MB-231 or MDA-MB-453 cells were examined for invadopodia extension for 6 h in 3.0-μm porous Boyden chamber membranes coated with vehicle (*Uncoated*) or type IV collagen on upper sides (*Upper*), both sides (*Both*), or lower sides (*Lower*). Invadopodia on the lower sides of the membrane were stained with cortactin antibodies and counted per field of the microscope. *Bar*, 10 μm. Objective lens, magnification, ×40; numerical aperture, 0.95. *C*, DAAM1 silence significantly inhibited collagen-induced invadopodia extension. Stable DAAM1 knockdown MDA-MB-231 cells (DAAM1 shRNA #1 and #2) or control cells were allowed to extend invadopodia for 6 h. The number of extended invadopodia was determined by 3.0-μm porous Boyden chamber assays and counted per field of the microscope. *D*, cyclo(-RGDfK) suppressed collagen-induced invadopodia extension. MDA-MB-231 cells were treated with 20 nmol/liter cyclo(-RGDfK) or vehicle and allowed to extend invadopodia for 6 h. The number of extended invadopodia was determined by 3.0-μm porous Boyden chamber assays and counted per field of the microscope. *E*, DAAM1 silence or cyclo(-RGDfK) significantly inhibited collagen-induced invadopodia extension. MDA-MB-453 cells transfected with DAAM1 shRNA or treated with cyclo(-RGDfK) were allowed to extend invadopodia for 6 h. The number of extended invadopodia was determined by 3.0-μm porous Boyden chamber assays and counted per field of the microscope. *Bo*, collagen coated on both sides. *Lo*, collagen coated on the lower sides. *F–H*, abundant active DAAM1 were located in invadopodia. MDA-MB-231 or MDA-MB-453 cells were seeded on 3.0-μm porous Boyden chamber membranes coated with collagen type IV on the lower sides. The invadopodia of MDA-MB-231 or MDA-MB-453 cells were allowed to extend toward collagen for 4 h. Cell bodies and invadopodia were separated as described under "Experimental procedures." Cellular lysates were assayed for the active DAAM1 by a pulldown assay using a GST-RHOA as a bait. *Error bars*, S.D.

regulation of the cell migration and organization of the intracellular cytoskeleton (23). Actin remodeling and cell movement are triggered via rapid signaling to integrin $\alpha v\beta3$, Src, phosphatidylinositol 3-OH kinase, and focal adhesion kinase in breast cancer T-47D cells (14). Integrin $\beta3$ also could employ the phosphatidylinositol 3-OH kinase–Akt and the MAPK pathway for enabling cell survival and proliferation in MDA-MB-231 cells (24). Integrin $\beta3$ participates in invadopodia

formed by lung carcinoma cells, and it is associated with poor prognosis and increased metastasis in lung cancer (25). The MENA-mediated haptotactic response in breast cancer cells depends on MENA's binding to $\alpha5\beta1$ integrin receptor, adhesion protein signaling, and fibronectin fibrillogenesis (26, 27). In this study, we find that integrin $\alpha v\beta3$ associating with, but indirectly binding to, the C-terminal DAD domain of DAAM1 promotes collagen-induced haptotaxis of breast cancer cells.
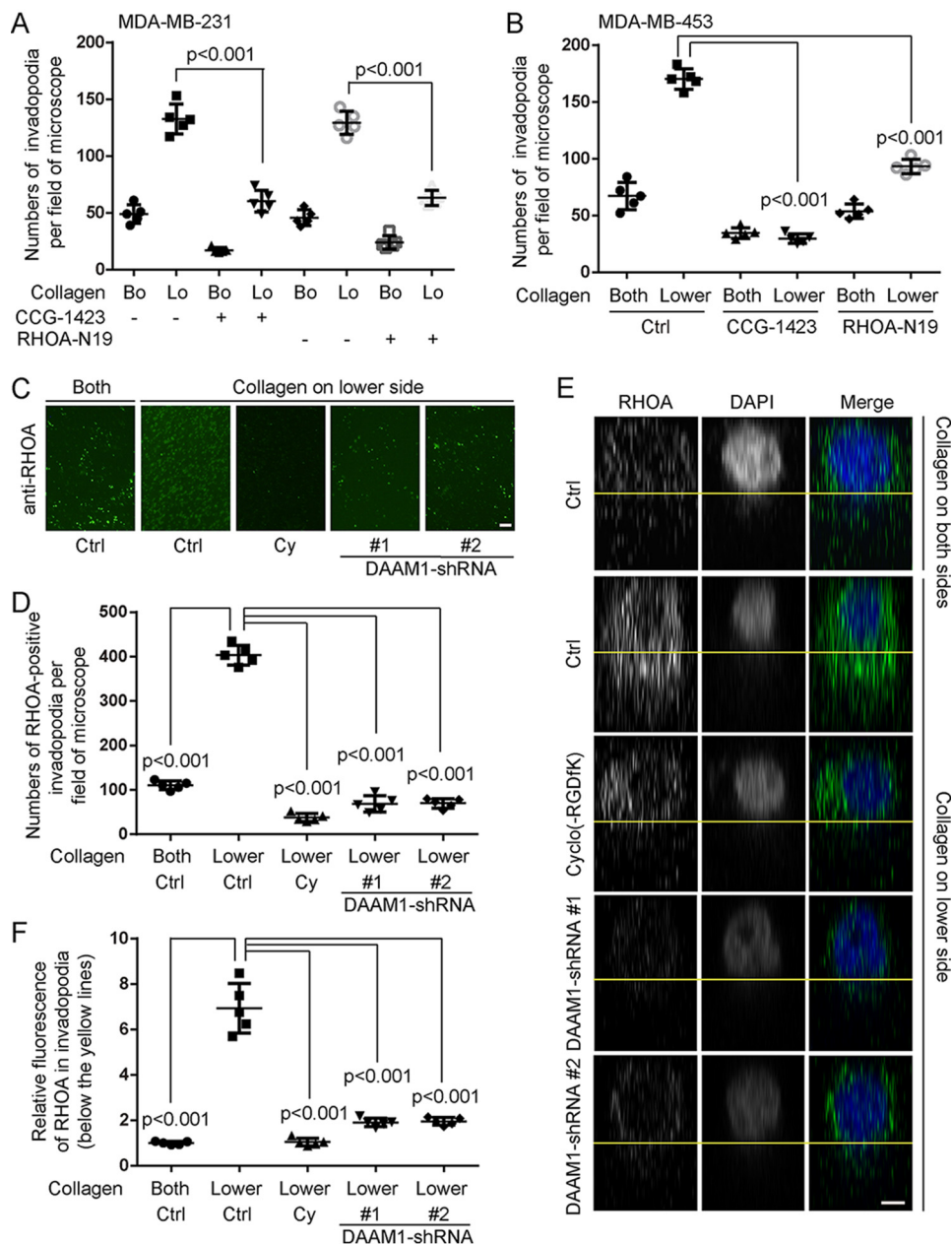
Figure 5. DAAM1-dependent activation of RHOA mediates collagen-induced invadopodia extension. *A*, blockade of RHOA inhibited collagen-induced invadopodia extension of MDA-MB-231 cells. MDA-MB-231 cells treated with CCG-1423 (RHOA-specific inhibitor, 1 μmol/liter) or RHOA-N19 overexpressing stable MDA-MB-231 cells were seeded in 3.0-μm porous Boyden chamber membranes coated with type IV collagen on both sides (*Bo*) or on the lower sides (*Lo*). Cells were allowed to extend invadopodia toward collagen for 6 h. The number of extended invadopodia were counted per field of the microscope. *B*, blockade of RHOA inhibited collagen-induced invadopodia extension of MDA-MB-453 cells. MDA-MB-453 cells treated with CCG-1423 (1 μmol/liter) or transfected with RHOA-N19 were seeded on 3.0-μm porous Boyden chamber membranes coated with type IV collagen on both sides (*Both*) or on the lower sides (*Lower*). Cells were allowed to extend invadopodia toward collagen for 6 h. The number of extended invadopodia were counted per field of the microscope. *C*, *D*, *E*, and *F*, the high expression of RHOA in invadopodia was disrupted by cyclo(-RGDfK) treatment or DAAM1 knockdown. MDA-MB-231 cells treated with cyclo(-RGDfK) (20 nmol/liter) or stable DAAM1 knockdown MDA-MB-231 cells were seeded on 3.0-μm porous Boyden chamber membranes coated with type IV collagen on both sides (*Both*) or on the lower sides (*Lower*). Cells were allowed to extend invadopodia toward collagen for 6 h. *Cy*, cyclo(-RGDfK). Invadopodia on the lower sides of the membrane were stained with RHOA antibodies and counted per field of the microscope. *C* and *D*, the expression and location of RHOA in invadopodia are shown on the lower sides of 3.0-μm porous Boyden chamber membranes. The number of RHOA-positive invadopodia were counted per field of the microscope. *Bar*, 10 μm. Objective lens, magnification, $\times$40; numerical aperture, 0.95. *E* and *F*, z-axis scan of 3.0-μm pores in Boyden chamber membranes. The fluorescence of RHOA (*green*) in invadopodia (*below* the *yellow lines*) was adjusted by ZEN software and normalized to the average value of control groups. Objective lens, magnification, $\times$63; numerical aperture, 1.4. $n = 5$. z-Distance $= 16$ μm. *Bar*, 1 μm. Pixel dimensions are 99×66 pixels. *Error bars*, S.D.

Invadopodia, actin-rich protrusions anchoring the plasma membrane, can decompose ECM during cancer invasiveness and metastasis (15). In this study, we test the ability of DAAM1 to stimulate invadopodia extension in Boyden chambers (a three-dimensional cell culture system). Its two chambers offer different chemical environments in which cell migration can be stimulated. Cell haptotactic migration can be imitated simply by adding soluble chemoattractants into the bottom compartment or coating the lower membrane with ECM proteins (28). Our Boyden chamber assays show that integrin $\alpha v \beta 3$ inhibitor
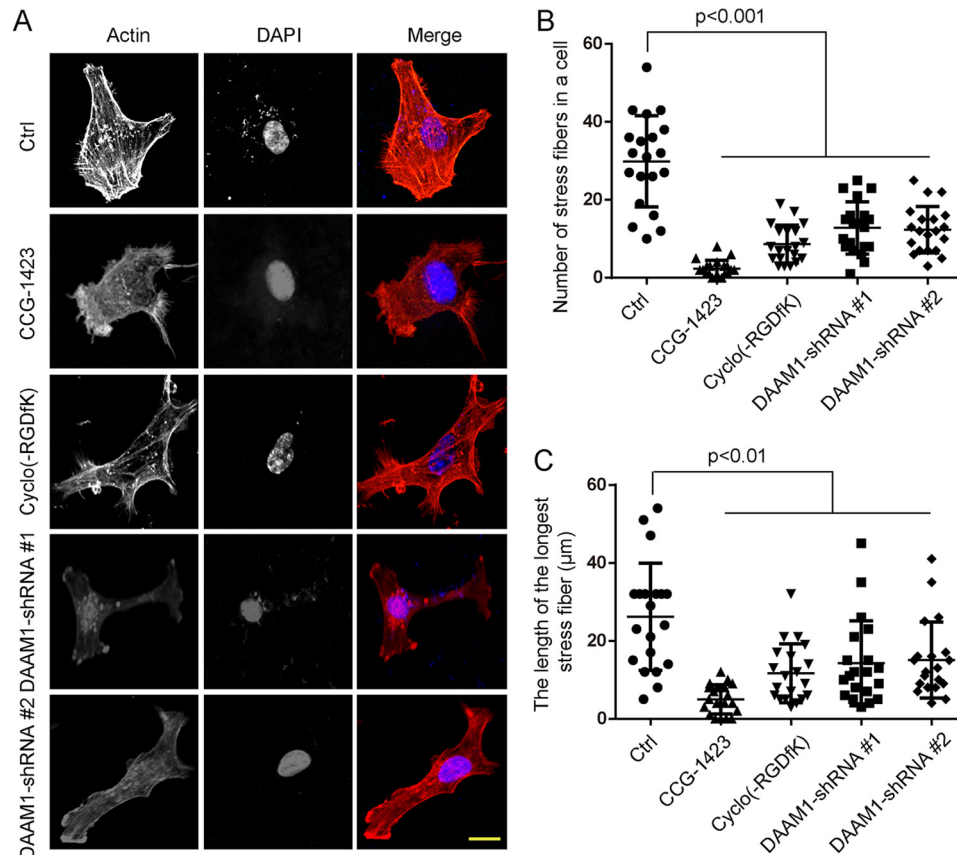
Figure 6. DAAM1 and RHOA participate in the rearrangement of stress fibers. *A*, DAAM1 shRNA, CCG-1423 treatment, or cyclo(-RGDfK) treatment disrupted the formation of actin stress fibers in MDA-MB-231 cells. Stable DAAM1 knockdown MDA-MB-231 cells were grown on collagen-coated coverslips. MDA-MB-231 cells grown on collagen-coated coverslips were pretreated with 1 μmol/liter CCG-1423 or 20 nmol/liter cyclo(-RGDfK) for 1 h. Subsequently, cells were fixed, and F-actin organization was analyzed by phalloidin staining. *Bar*, 10 μm. Objective lens, magnification, ×40; numerical aperture, 0.95. *B* and *C*, DAAM1 shRNA, CCG-1423, or cyclo(-RGDfK) disrupted the formation of stress fibers in MDA-MB-231 cells. The number of stress fibers in a cell (*B*) and the length of the longest microfilament (*C*) were determined in MDA-MB-231 cells ($n = 20$). *Error bars*, S.D.

or DAAM1 knockdown blocks collagen-induced invadopodia extension.

DAAM1 and Rho GTPases cooperatively regulate the signaling pathways, being responsible for the dynamics of actin filaments (18, 19, 29). Two type of actin assembly factors, DAAM1 and mDia1, exhibit distinct efficiencies when directly regulated by Rho GTPases (30). Aspenström *et al.* (29) reported that their study's results are not consistent with a model in which DAAM1 activates RHOA; instead, the protein is likely to be a downstream effector of RHOA. Here, we were unable to detect any collagen-induced activation of DAAM1 with the nucleotide-free mutant RHOA-N19. N-DAAM1 largely retarded the haptotaxis of breast cancer cells, which could be rescued by constitutively active RHOA (RHOA-V14) overexpression. This study concludes that RHOA acts as a downstream target of integrin $\alpha v\beta 3$/DAAM1 and mediates collagen-induced stress fiber formation and haptotaxis of breast cancer cells. On the contrary, WAVE complex brings high motility to the membranes of junctions in epithelial cells, but DAAM1-mediated actin regulation restrains this motility (31). Guillabert-Gourgues *et al.* (20) report that Kif26b and DAAM1 cooperatively regulate the initiation of epithelial cells' sprouting and their directional migration via microtubule reorganization. Bile acid stimulates haptotaxis in colorectal cancer cells via the RHOA/Rho-kinase pathway and signaling cascades, including protein

kinase C, mitogen-activated protein kinase, and cyclooxygenase-2 (32). For the first time, our study determines the importance of the integrin $\alpha v\beta 3$/DAAM1/RHOA signaling pathway in maintaining stress fiber formation and cell haptotaxis for breast cancer metastasis.

Although this study offers a mechanistic understanding on the role of DAAM1 in cancer cell migration, how DAAM1 precisely regulates haptotaxis and motility of breast cancer cells has yet to be determined. Together, our data prove the effectiveness of the integrin $\alpha v\beta 3$/DAAM1/RHOA-dependent mechanism that leads to increased collagen-induced invadopodia extension and haptotaxis of breast cancer cells. These findings elucidate a molecular pathway linking integrin $\alpha v\beta 3$/DAAM1 signaling with invadopodia extension and cell haptotaxis, which may shed new light on the invasive and metastatic mechanisms of breast cancer.

Experimental procedures

Cell culture and transfections

MDA-MB-231, MDA-MB-453, HEK-293T, and MCF10A cell lines were purchased from the Cell Bank of the Chinese Academy of Sciences (Shanghai, China). MDA-MB-231, MDA-MB-453, and HEK-293T cells were grown in Dulbecco's modified Eagle's medium (high-glucose) (catalog no. SH30022.01,

~SASBMB

J. Biol. Chem. (2018) 293(26) 10172–10185 **10181**

Hyclone, Logan, UT) supplemented with 10% (v/v) fetal bovine serum (catalog no. SH30068.03, Hyclone) in a humidified incubator at 37 °C with 5% CO_2. MCF10A cells were grown in Dulbecco's modified Eagle's medium/F-12 medium (catalog no. 12500096, Gibco) supplemented with 5% (v/v) horse serum (catalog no. SH30074.03, Hyclone), 20 ng/ml human EGF, 10 μg/ml insulin, 0.5 μg/ml hydrocortisone, penicillin, streptomycin, and 100 ng/ml cholera toxin. All cell lines were verified monthly to be mycoplasma-negative.

The constructs of N-DAAM1 (N terminus of DAAM1), C-DAAM1 (C terminus of DAAM1), ΔDAD-DAAM1 (DAAM1 lacking the DAD (Diaphanous-like autoregulatory domain) domain), RHOA-V14 (constitutively active RHOA), and RHOA-N19 (dominant-negative RHOA) were previously generated by our laboratory (19, 33). For the construct of the GST-tagged integrin β3 cytoplasmic tail, the fragment of the integrin β3 tail (amino acids 716–762) was amplified by PCR and inserted into pGEX-6p-1 vector (34). The cells were seeded in 6-well plates (Costar, Corning, Inc.) and cultured to 80–90% confluence and then transfected with plasmids (4 μg/well) using Lipofectamine 2000 reagent (10 μl/well) (catalog no. 11668-019, Invitrogen) in serum-free Opti-MEM. The cells were switched to fresh medium containing 10% fetal bovine serum 6 h after the transfection and cultured for 48 h.

The targeting sequences of the shRNAs are as follows: DAAM1 #1 (5′-GCCACTTTGTATCCTATCAGG-3′) and DAAM1 #2 (5′-GCAGGATTTCTTTGTGAACAG-3′). The shRNAs were designed and cloned into Tet-pLKO-puro vector (a kind gift from Dr. Yu Jiang, University of Pittsburgh). The resulting plasmids were transfected into MDA-MB-231 and MDA-MB-453 cells using Lipofectamine 2000 reagent (catalog no. 11668-019, Invitrogen) and selected against puromycin. Clones stably expressing the doxycycline-inducible shRNAs were isolated. The inducible cells were cultured in the presence of puromycin (1 μg/ml), and the expression of shRNA was induced by including 100 ng/ml doxycycline in the culture medium. All cells were maintained in a 37 °C incubator with 5% CO_2 and cultured as the parental cells.

Boyden chamber assays

Cell migration was assessed in a modified Boyden chamber system (Costar, Corning, NY), in which the two chambers were separated by a polycarbonate membrane (8.0-μm pore diameter) (catalog no. 3422, Costar). For invadopodia extension, Boyden chamber membranes with 3.0-μm pores (catalog no. 3415, Costar) were employed. The lower side or two sides of Boyden chamber membranes were coated with human type IV collagen (10 μg/ml) (Sigma-Aldrich) for 2 h at 37 °C. MDA-MB-231, MDA-MB-453, or MCF10A cells were grown to subconfluence in tissue culture plates, detached, centrifuged, and rendered into single cell suspensions in serum-free culture medium supplemented with 5 μg/ml BSA. The suspensions containing 1×10^5 cells were added to wells with a membrane placed at the bottom. The cells were allowed to migrate or extend invadopodia for the indicated periods of time at 37 °C. Thereafter, the medium was discarded, stationary cells were removed with a cotton-tipped applicator, and the membranes were cut off of the chamber and stained with 0.5% crystal violet or the indicated fluorescently labeled antibodies. The response was evaluated in a microscope (Mshot MF53, Micro-shot Technology Co., Guangzhou, China) by counting the number of cells or invadopodia that had passed through the membrane.

Migrating cells, invadopodia, and cell body isolation

Cells were seeded on the upper surface of the Boyden chamber membranes (8.0-μm pores) and allowed to migrate into the bottom chamber. Nonmigrating cells remained on the upper sides of membranes and were manually removed with a cotton swab. Migrating cells were adhered onto the lower sides of membranes and scraped into lysis buffer as described below.

To isolate invadopodia and cell bodies of cells induced to migrate with collagen, we followed the protocol described previously with some modifications (28, 35, 36). Cells were seeded on the upper surface of the Boyden chamber membranes (3.0-μm pores) and allowed invadopodia to extend into the bottom chamber. After the indicated time, the cells were briefly rinsed with PBS and fixed with 0.3% methanol-free formaldehyde in PBS for 10 min at room temperature. Glycine was added to 250 mmol/liter for 5 min at room temperature, and the cells were washed twice with PBS. To isolate invadopodia, cell bodies on the upper sides of the membrane surface were manually removed with a cotton swab and laboratory paper, and invadopodia on the lower sides of the membranes were scraped into cross-link reversal buffer (100 mmol/liter Tris, pH 6.8, 5 mmol/liter EDTA, 10 mmol/liter DTT, and 1% SDS). Cell bodies were similarly isolated except that invadopodia on the lower sides of the membranes were manually removed, and cell bodies were scraped into cross-link reversal buffer. Extracts were incubated at 70 °C for 45 min to reverse the formaldehyde-induced cross-links.

Immunoblotting

Cells grown in Boyden chambers were washed twice with PBS and then lysed with ice-cold radioimmune precipitation assay lysis buffer (50 mmol/liter Tris, 150 mmol/liter NaCl, 1% Triton X-100, 1% sodium deoxycholate, 0.1% SDS, 1 mmol/liter sodium orthovanadate, 1 mmol/liter sodium fluoride, 1 mmol/liter EDTA, 1 mmol/liter PMSF, and 1% mixture of protease inhibitors) (pH 7.4). The lysates were then clarified by centrifugation at $12,000 \times g$ for 20 min at 4 °C. An equal amount of protein extracts were separated by 8 or 10% SDS-PAGE. The following antibodies were used: anti-integrin β3 (1:1000 dilution; catalog no. 18309-1-AP, ProteinTech Group, Wuhan, China), anti-GAPDH (1:5000 dilution; catalog no. 60004-1-Ig, ProteinTech), anti-β-actin (1:5000 dilution; catalog no. 60008-1-Ig, ProteinTech), anti-histone H3 (1:5000 dilution; catalog no. 17168-1-AP, ProteinTech), anti-HA tag (1:2000 dilution; catalog no. 51064-2-AP, ProteinTech), anti-DAAM1 (1:1000 dilution; catalog no. sc-100942, Santa Cruz Biotechnology, Inc.), and anti-cortactin (1:2000 dilution; catalog no. ab81208, Abcam) antibodies. Protein bands were detected after incubation with horseradish peroxidase– conjugated antibodies and visualized with Pierce™ ECL Western blotting Substrate (catalog no. 32209, Thermo Scientific, Rockford, IL).

Pulldown assays

For detection of active DAAM1, GST-RHOA beads were incubated with 0.1 mmol/liter GTPγS (Sigma-Aldrich) at 30 °C for 15 min with constant agitation. Cells grown in Boyden chambers were washed twice with PBS and then lysed with lysis buffer containing 1% Triton X-100, 50 mmol/liter HEPES, pH 7.4, 140 mmol/liter NaCl, 1 mmol/liter EDTA, 1 mmol/liter PMSF, and 1× protease inhibitor mixture. Equal amounts of total cellular protein were incubated with GTPγS-incubated GST-RHOA beads captured on MagneGST GSH particles (Promega, Madison, WI) at 4 °C with constant rotation for 90 min. The beads were washed three times with washing buffer (4.2 mmol/liter Na_2HPO_4, 2 mmol/liter KH_2PO_4, 280 mmol/liter NaCl, and 10 mmol/liter KCl, pH 7.2). At the end of this period, beads were captured by magnet in a magnetic stand.

For an *in vitro* binding assay, GST-tagged integrin β3 tail (amino acids 716–762) was purified by using GSH-Sepharose 4B (catalog no. 17-0756-01, GE Healthcare, Uppsala, Sweden). HA-tagged full-length DAAM1 was purified by using Pierce anti-HA agarose (catalog no. 26181, Thermo Scientific). The beads were washed three times with washing buffer and captured by centrifugation at 12,000 × g for 5 min.

After washing with ice-cold buffer three times, beads were resuspended in Laemmli buffer, boiled, and subjected to immunoblotting analysis. SDS-PAGE and immunoblotting were performed using standard methods.

Immunoprecipitation

To test interaction between DAAM1 and integrin, cells were lysed with lysis buffer containing 50 mmol/liter HEPES, pH 7.4, 100 mmol/liter NaCl, 1 mmol/liter EDTA, 1% Triton X-100, 1 mmol/liter phenylmethylsulfonyl fluoride, and 1× protease inhibitor mixture. Cell debris and unbroken cells were removed by centrifugation at 10,000 × g for 10 min. Clarified lysates were incubated with antibodies overnight followed by the addition of protein A/G-conjugated agarose beads (Pierce). After incubation for an additional 1.5 h with agitation, beads were washed four times with lysis buffer, once with 20 mmol/liter Tris-HCl (pH 7.4), and boiled for 5 min in 60 liters of 2× SDS sample buffer. Samples were subjected to SDS-PAGE and blotted with anti-integrin β3 (1:1000 dilution) or anti-DAAM1 antibodies (1:1000 dilution).

HEK-293T cells were transfected with the indicated constructs of HA-tagged DAAM1. After 24 h, cell lysates were harvested and incubated with anti-HA antibody and protein A/G-conjugated agarose beads at 4 °C with constant rotation overnight. The immunoprecipitates were analyzed by immunoblotting with anti-HA (1:2000 dilution) or anti-integrin β3 antibodies (1:1000 dilution). Whole-cell lysates were used as controls.

Rho GTPase activation assays (G-LISA small GTPase activation assays)

In Rho GTPase (RHOA, CDC42, and RAC1) activation assays (catalog nos. BK121 for RHOA, BK127 for CDC42, and BK126 for RAC1, Cytoskeleton Inc., Denver, CO), MDA-MB-231, MDA-MB-453, or stable DAAM1 knockdown MDA-MB-231 cells were seeded onto Boyden chambers with the lower sides of membranes coated with human type IV collagen. Cells were allowed to migrate for 4 h. Then equal volumes of total cellular protein extracted from Boyden chambers were subjected to Rho GTPase activation assays. The experiments were then performed according to the manufacturer's protocol.

G-LISA small GTPase activation assays offer a fast and sensitive method for performing small G-protein activation assays. Briefly, equal protein concentration in all samples is a prerequisite for accurate comparison between samples in GTPase activation assays. Cell extracts were equalized with ice-cold lysis buffer containing protease inhibitor mixture to give identical protein concentrations. The G-LISA small GTPase activation assay is a simple one-step procedure that results in a red-to-purple/blue color change characterized by an increase in absorbance at 600 nm. Ten μl of each lysate or lysis buffer is pipetted into a 96-well plate, followed by 290 μl of Precision Red Advanced Protein Assay Reagent. The mixture is incubated for 1 min at room temperature. A spectrophotometer is used to measure the photometric intensity of 290 μl of Precision Red plus 10 μl of lysis buffer at 600 nm. Then the absorbance of lysate samples is read.

Immunofluorescence and actin cytoskeleton staining

Invadopodia and cell bodies adhering to Boyden chamber membranes were fixed in 4% paraformaldehyde in PBS for 20 min, permeabilized in 0.2% Triton X-100, and blocked in PBS containing 1% BSA for 60 min at room temperature. Next, invadopodia and cell bodies were incubated with anti-RHOA (1:100 dilution; catalog no. 10749-1-AP, ProteinTech Group) antibodies for 1 h at room temperature and then treated with FITC-labeled secondary antibodies (Sigma-Aldrich) for 1 h at room temperature. To account for the number of invadopodia extended, invadopodia on the lower sides of Boyden chamber membranes (3.0-μm pores) were stained with anti-cortactin (1:100 dilution; catalog no. ab81208, Abcam) for 1 h at room temperature and then treated with FITC-labeled secondary antibodies (Sigma-Aldrich) for 1 h at room temperature. For the actin cytoskeleton staining assay, cells were grown on glass slides and stained with TRITC-labeled phalloidin (5 μg/ml; Sigma-Aldrich) or anti-myosin II (1:200 dilution; catalog no. 10609-1-AP, Protein-Tech Group) for 40 min at room temperature and then treated with FITC-labeled secondary antibodies (Sigma-Aldrich) for 1 h at room temperature. After washing with PBS, the membranes were mounted on glass slides with DAPI Fluoromount G (Southern Biotech, Birmingham, AL). The images were acquired with a fluorescence microscope (LSM710, Zeiss, Oberkochen, Germany). To assess invadopodia extension, images were acquired in *z*-axis for a fluorescence scan. The fluorescence intensity and assembled *z*-axis images were analyzed and merged by ZEN software (Zeiss).

Statistical analysis

All statistical analyses were done using SPSS version 23.0 software (Chicago, IL). Most of the data were analyzed by one-

way analysis of variance or Student's *t* test. Scatter plot charts show scatter plots and means ± S.D. of six independent experiments if not noted. For all analyses, a two-sided *p* value of <0.05 was deemed statistically significant.

References

1. McCarthy, J. B., Palm, S. L., and Furcht, L. T. (1983) Migration by haptotaxis of a Schwann cell tumor line to the basement membrane glycoprotein laminin. *J. Cell Biol.* **97,** 772–777 CrossRef Medline

2. Santiago-Medina, M., and Yang, J. (2016) MENA promotes tumor-intrinsic metastasis through ECM remodeling and haptotaxis. *Cancer Discov.* **6,** 474–476 CrossRef Medline

3. Hynes, R. O. (2014) Stretching the boundaries of extracellular matrix research. *Nat. Rev. Mol. Cell Biol.* **15,** 761–763 CrossRef Medline

4. Charras, G., and Sahai, E. (2014) Physical influences of the extracellular environment on cell migration. *Nat. Rev. Mol. Cell Biol.* **15,** 813–824 CrossRef Medline

5. Hynes, R. O. (2009) The extracellular matrix: not just pretty fibrils. *Science* **326,** 1216–1219 CrossRef Medline

6. Jacob, A., and Prekeris, R. (2015) The regulation of MMP targeting to invadopodia during cancer metastasis. *Front. Cell Dev. Biol.* **3,** 4 Medline

7. Demircioglu, F., and Hodivala-Dilke, K. (2016) αvβ3 integrin and tumour blood vessels: learning from the past to shape the future. *Curr. Opin. Cell Biol.* **42,** 121–127 CrossRef Medline

8. Zeltz, C., and Gullberg, D. (2016) The integrin-collagen connection: a glue for tissue repair? *J. Cell Sci.* **129,** 1284 CrossRef Medline

9. Moilanen, J. M., Löffek, S., Kokkonen, N., Salo, S., Väyrynen, J. P., Hurskainen, T., Manninen, A., Riihilä, P., Heljasvaara, R., Franzke, C. W., Kähäri, V. M., Salo, T., Mäkinen, M. J., and Tasanen, K. (2017) Significant role of collagen XVII and integrin β4 in migration and invasion of the less aggressive squamous cell carcinoma cells. *Sci. Rep.* **7,** 45057 CrossRef Medline

10. Lu, Y. Y., Lin, Y. K., Kao, Y. H., Chung, C. C., Yeh, Y. H., Chen, S. A., and Chen, Y. J. (2016) Collagen regulates transforming growth factor-β receptors of HL-1 cardiomyocytes through activation of stretch and integrin signaling. *Mol. Med. Rep.* **14,** 3429–3436 CrossRef Medline

11. Pécheur, I., Peyruchaud, O., Serre, C. M., Guglielmi, J., Voland, C., Bourre, F., Margue, C., Cohen-Solal, M., Buffet, A., Kieffer, N., and Clézardin, P. (2002) Integrin α(v) β3 expression confers on tumor cells a greater propensity to metastasize to bone. *FASEB J.* **16,** 1266–1268 CrossRef Medline

12. Galliher, A. J., and Schiemann, W. P. (2006) β3 integrin and Src facilitate transforming growth factor-β mediated induction of epithelial-mesenchymal transition in mammary epithelial cells. *Breast Cancer Res.* **8,** R42 CrossRef Medline

13. Li, W., Liu, C., Zhao, C., Zhai, L., and Lv, S. (2016) Downregulation of β3 integrin by miR-30a-5p modulates cell adhesion and invasion by interrupting Erk/Ets1 network in triple-negative breast cancer. *Int. J. Oncol.* **48,** 1155–1164 CrossRef Medline

14. Flamini, M. I., Uzair, I. D., Pennacchio, G. E., Neira, F. J., Mondaca, J. M., Cuello-Carrión, F. D., Jahn, G. A., Simoncini, T., and Sanchez, A. M. (2017) Thyroid hormone controls breast cancer cell movement via integrin αV/β3/SRC/FAK/PI3-kinases. *Horm. Cancer* **8,** 16–27 CrossRef Medline

15. Murphy, D. A., and Courtneidge, S. A. (2011) The "ins" and "outs" of podosomes and invadopodia: characteristics, formation and function. *Nat. Rev. Mol. Cell Biol.* **12,** 413–426 CrossRef Medline

16. Kerkhoff, E. (2011) Actin dynamics at intracellular membranes: the Spir/formin nucleator complex. *Eur. J. Cell Biol.* **90,** 922–925 CrossRef Medline

17. Schönichen, A., and Geyer, M. (2010) Fifteen formins for an actin filament: a molecular view on the regulation of human formins. *Biochim. Biophys. Acta* **1803,** 152–163 CrossRef Medline

18. Habas, R., Kato, Y., and He, X. (2001) Wnt/Frizzled activation of Rho regulates vertebrate gastrulation and requires a novel Formin homology protein Daam1. *Cell* **107,** 843–854 CrossRef Medline

19. Zhu, Y., Tian, Y., Du, J., Hu, Z., Yang, L., Liu, J., and Gu, L. (2012) Dvl2-dependent activation of Daam1 and RhoA regulates Wnt5a-induced breast cancer cell migration. *PLoS One* **7,** e37823 CrossRef Medline

20. Guillabert-Gourgues, A., Jaspard-Vinassa, B., Bats, M. L., Sewduth, R. N., Franzl, N., Peghaire, C., Jeanningros, S., Moreau, C., Roux, E., Larrieu-Lahargue, F., Dufourcq, P., Couffinhal, T., and Duplàa, C. (2016) Kif26b controls endothelial cell polarity through the Dishevelled/Daam1-dependent planar cell polarity-signaling pathway. *Mol. Biol. Cell* **27,** 941–953 CrossRef Medline

21. Ridley, A. J. (2015) Rho GTPase signalling in cell migration. *Curr. Opin. Cell Biol.* **36,** 103–112 CrossRef Medline

22. Liu, W., Sato, A., Khadka, D., Bharti, R., Diaz, H., Runnels, L. W., and Habas, R. (2008) Mechanism of activation of the Formin protein Daam1. *Proc. Natl. Acad. Sci. U.S.A.* **105,** 210–215 CrossRef Medline

23. Kwakwa, K. A., and Sterling, J. A. (2017) Integrin αvβ3 signaling in tumor-induced bone disease. *Cancers* **9,** E84 Medline

24. Nair, M. G., Desai, K., Prabhu, J. S., Hari, P. S., Remacle, J., and Sridhar, T. S. (2016) β3 integrin promotes chemoresistance to epirubicin in MDA-MB-231 through repression of the pro-apoptotic protein, BAD. *Exp. Cell Res.* **346,** 137–145 CrossRef Medline

25. Peláez, R., Morales, X., Salvo, E., Garasa, S., Ortiz de Solórzano, C., Martínez, A., Larrayoz, I. M., and Rouzaut, A. (2017) β3 integrin expression is required for invadopodia-mediated ECM degradation in lung carcinoma cells. *PLoS One* **12,** e0181579 CrossRef Medline

26. Oudin, M. J., Jonas, O., Kosciuk, T., Broye, L. C., Guido, B. C., Wyckoff, J., Riquelme, D., Lamar, J. M., Asokan, S. B., Whittaker, C., Ma, D., Langer, R., Cima, M. J., Wisinski, K. B., Hynes, R. O., *et al.* (2016) Tumor cell-driven extracellular matrix remodeling drives haptotaxis during metastatic progression. *Cancer Discov.* **6,** 516–531 CrossRef Medline

27. Oudin, M. J., Miller, M. A., Klazen, J. A., Kosciuk, T., Lussiez, A., Hughes, S. K., Tadros, J., Bear, J. E., Lauffenburger, D. A., and Gertler, F. B. (2016) MenaINV mediates synergistic cross-talk between signaling pathways driving chemotaxis and haptotaxis. *Mol. Biol. Cell* **27,** 3085–3094 CrossRef Medline

28. Mili, S., Moissoglu, K., and Macara, I. G. (2008) Genome-wide screen reveals APC-associated RNAs enriched in cell protrusions. *Nature* **453,** 115–119 CrossRef Medline

29. Aspenström, P., Richnau, N., and Johansson, A. S. (2006) The diaphanous-related formin DAAM1 collaborates with the Rho GTPases RhoA and Cdc42, CIP4 and Src in regulating cell morphogenesis and actin dynamics. *Exp. Cell Res.* **312,** 2180–2194 CrossRef Medline

30. Higashi, T., Ikeda, T., Shirakawa, R., Kondo, H., Kawato, M., Horiguchi, M., Okuda, T., Okawa, K., Fukai, S., Nureki, O., Kita, T., and Horiuchi, H. (2008) Biochemical characterization of the Rho GTPase-regulated actin assembly by diaphanous-related formins, mDia1 and Daam1, in platelets. *J. Biol. Chem.* **283,** 8746–8755 CrossRef Medline

31. Nishimura, T., Ito, S., Saito, H., Hiver, S., Shigetomi, K., Ikenouchi, J., and Takeichi, M. (2016) DAAM1 stabilizes epithelial junctions by restraining WAVE complex-dependent lateral membrane motility. *J. Cell Biol.* **215,** 559–573 CrossRef Medline

32. Debruyne, P. R., Bruyneel, E. A., Karaguni, I. M., Li, X., Flatau, G., Müller, O., Zimber, A., Gespach, C., and Mareel, M. M. (2002) Bile acids stimulate invasion and haptotaxis in human colorectal cancer cells through activation of multiple oncogenic signaling pathways. *Oncogene* **21,** 6740–6750 CrossRef Medline

ASBMB

33. Liu, J., Zhang, Y., Xu, R., Du, J., Hu, Z., Yang, L., Chen, Y., Zhu, Y., and Gu, L. (2013) PI3K/Akt-dependent phosphorylation of GSK3β and activation of RhoA regulate Wnt5a-induced gastric cancer cell migration. *Cell. Signal.* **25,** 447–456 CrossRef Medline

34. Ma, Y. Q., Qin, J., Wu, C., and Plow, E. F. (2008) Kindlin-2 (Mig-2): a co-activator of β3 integrins. *J. Cell Biol.* **181,** 439–446 CrossRef Medline

35. Cho, S. Y., and Klemke, R. L. (2002) Purification of pseudopodia from polarized cells reveals redistribution and activation of Rac through assembly of a CAS/Crk scaffold. *J. Cell Biol.* **156,** 725–736 CrossRef Medline

36. Wang, Y., Ding, S. J., Wang, W., Yang, F., Jacobs, J. M., Camp, D., 2nd, Smith, R. D., and Klemke, R. L. (2007) Methods for pseudopodia purification and proteomic analysis. *Sci. STKE* **2007,** pl4 Medline

≋ASBMB

J. Biol. Chem. (2018) 293(26) 10172–10185 **10185**